LBL-30847
Preprint

Lawrence Berkeley Laboratory
UNIVERSITY OF CALIFORNIA

Submitted to Physical Review C

Direct Observation of the Giant Dipole Resonance of ^{16}O via Electromagnetic Dissociation

D.L. Olson, M. Baumgartner, D.E. Greiner, P.J. Lindstrom,
T.J.M. Symons, R. Wada, M.L. Webb, B.L. Berman,
H.J. Crawford, and J.M. Engelage

June 1991

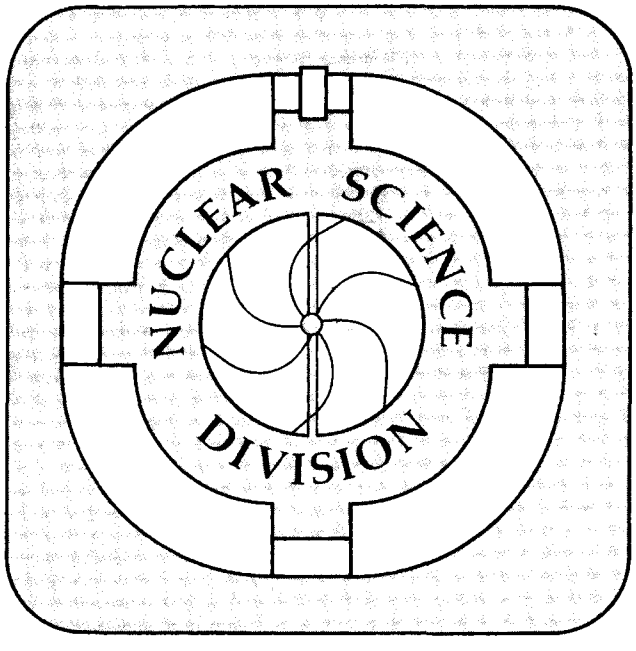

Prepared for the U.S. Department of Energy under Contract Number DE-AC03-76SF00098

DISCLAIMER

LBL-30847

Submitted to Physical Review C

Direct Observation of the Giant Dipole Resonance of ^{16}O via Electromagnetic Dissociation

D.L. Olson, M. Baumgartner, D.E. Greiner, P.J. Lindstrom, T.J.M. Symons,
R. Wada, and M.L. Webb
Nuclear Science Division, Lawrence Berkeley Laboratory
University of California, Berkeley, CA 94720

B.L. Berman
Center for Nuclear Studies, The George Washington University,
Washington D. C. 20052

H.J. Crawford and J.M. Engelage
University of California, Space Sciences Laboratory
Berkeley, CA 94720

June 1991

This work was supported by the Director, Office of Energy Research, Division of Nuclear Physics of the Office of High Energy and Nuclear Physics of the U.S. Department of Energy under Contract DE-AC03-76SF00098

Direct Observation of the Giant Dipole Resonance of ^{16}O via Electromagnetic Dissociation

D. L. Olson, M. Baumgartner,[a] D. E. Greiner, P. J. Lindstrom,

T. J. M. Symons, R. Wada,[b] M. L. Webb
Lawrence Berkeley Laboratory,
Berkeley, CA 94720

B. L. Berman
Center for Nuclear Studies,
The George Washington University,
Washington DC 20052

H. J. Crawford and J. M. Engelage
University of California, Space Sciences Laboratory,
Berkeley, CA 94720

We have measured the invariant mass spectrum of the final state $^{15}N+p$ system in the reaction $T(^{16}O,^{15}N+p)X$ at 2.1 A GeV with Be, Cu, and U targets (T). Electromagnetic dissociation of the ^{16}O projectile nucleus in the Coulomb field of the target nucleus produces two prominent peaks in the proton-energy spectrum, one at 9 MeV, from transitions to the ground state of the residual ^{15}N nucleus, and the other at 4 MeV, from transitions to excited states. This is corroborated by γ rays corresponding to the de-excitation of the ^{15}N nucleus which are in coincidence with the 4-MeV peak and are suppressed for the 9-MeV peak. Nucleon-nucleus diffractive dissociation makes a significant contribution to the cross section and results in a peak at 1.5 MeV. Nucleon-nucleon quasi-elastic scattering results in a featureless high-energy tail above 20 MeV.

PACS Nos. 25.20,25.70

KEYWORDS:
NUCLEAR REACTIONS X(^{16}O,$^{15}N+p$), X=Be, Cu, U, E=2.1 GeV/nucleon; measured invariant mass spectra, deduced differential electromagnetic dissociation cross sections, deduced diffractive dissociation cross section, electromagnetic dissociation, diffractive dissociation, relativistic heavy ions.

---

[a] Present address: Hoffman-LaRoche, Basel, Switzerland.

[b] Present address: Texas A&M University, College Station, Texas, USA

I. INTRODUCTION

A. General

The electromagnetic dissociation (EMD) of relativistic heavy ions has been studied in inclusive-projectile,[1,2,3,4,5,6] exclusive-projectile[7] and target-fragmentation[8] experiments. In these experiments, integrated EMD cross sections have been measured. Here we report the first measurement of an exclusive differential EMD cross section, via a two-particle coincidence experiment, which permits us to extract information about the EMD process in much greater detail. In this investigation we had two primary objectives, 1) to perform a rigorous test of our understanding of the EMD process and 2) to determine the feasibility of utilizing EMD for photonuclear-reaction studies of both stable and β-unstable nuclei.

Our choice of experimental parameters for meeting these objectives is a beam of ^{16}O nuclei at 2.1 A GeV initiating the reaction $T(^{16}O,^{15}N+p)X$ for targets (T) of U, Cu, and Be. The ^{16}O nucleus has an advantage over any other as a result of the detailed photonuclear studies which have been carried out previously for this nucleus, by Caldwell et al.[9,10]. The measured cross sections for decays to the ^{15}N ground state, $\sigma(\gamma,p_o)$[11,12], and to excited states of $^{15}N_i$, $\sigma(\gamma,p_i)$[9,10], enable us to make a precise prediction of the proton energy spectrum generated by the EMD process.

As an additional verification of the EMD process, we used a NaI detector array to measure the de-excitation γ rays from the ^{15}N fragment. The EMD theory predicts two peaks in the proton energy spectrum (as measured in the projectile rest frame). A peak at about 9 MeV proton energy results from decays of the giant dipole resonance (GDR) in ^{16}O to the ground state of ^{15}N, and a peak at about 4 MeV proton energy results from GDR decays to excited states at 5-6 MeV in ^{15}N, which result in lower proton energies. These excited states in ^{15}N decay by emission of a γ ray which is in coincidence with a 4-MeV proton.

B. Kinematics

A detailed description of EMD is given in Ref. 2. In this discussion we utilize the notation of inverse kinematics, in which all of the kinematic variables are calculated in the rest frame of the projectile-fragment system. The basic idea is that the ^{16}O projectile nucleus absorbs a virtual photon from the Coulomb field of the target nucleus. This virtual photon, which is nearly purely transverse, excites the ^{16}O nucleus to a level with an energy equal to the virtual photon energy, ω, which then decays into an ^{15}N and a proton. The ^{15}N is produced either in its ground state or in an excited state with excitation energy E_i which subsequently decays by emitting one or more γrays.

By measuring the momentum of the projectile-frame charged particles we are able to reconstruct the invariant mass of the charged-particle final state, M. This is related to ω by

$$M = |\mathcal{P}_p + \mathcal{P}_N| = M_O + \omega - E_i = M_N + M_p + E^* \tag{1}$$

where M_O, M_N, and M_p are the rest masses of ^{16}O, ^{15}N, and the proton, respectively, $\mathcal{P}_p$ and $\mathcal{P}_N$ are the 4-momenta of the proton and ^{15}N, and E_i is the internal excitation energy of the ^{15}N. The excitation energy of the final state $^{15}N + p$ system is

$$E^* = \omega + Q - E_i \tag{2}$$

where Q is the Q-value for the reaction $^{16}O \rightarrow ^{15} N + p$.

The EMD cross section is calculated as the product of the virtual-photon spectrum, $N_\gamma(\omega)$, and one of the measured photoproton cross sections, $\sigma(\gamma, p)$[9,10,11,12],

$$\frac{d\sigma_{em}}{d\omega} = \sigma(\gamma, p) N_\gamma(\omega). \tag{3}$$

This is related to $d\sigma/dE_p$ as

$$\begin{aligned} \frac{d\sigma}{dE_p} &= \sum_{i=0}^{n} \frac{d\sigma_{em}^i}{d\omega} \frac{d\omega}{dE_p} \\ &= \sum_{i=0}^{n} \sigma(\gamma, p_i) N_\gamma(\omega) \frac{d\omega}{dE_p} \end{aligned} \tag{4}$$

where i denotes the state in ^{15}N, and

$$\frac{d\omega}{dE_p} = \frac{M_N + M_p}{M_N} \approx \frac{16}{15} \tag{5}$$

in the nonrelativistic limit. E_p is the inverse-kinematics equivalent to the proton energy measured in a normal-kinematics experiment.

II. EXPERIMENTAL SETUP AND ANALYSIS

This experiment was performed at the LBL HISS facility. A complete description of this facility is given in Ref. 13. A schematic diagram of the setup is shown in Fig. 1. The 2.1 A GeV ^{16}O beam is incident upon a set of plastic scintillation counters (TOF_1, TOT, HS, E) and drift chambers (DC_3, DC_4) before entering the main vacuum tank of the HISS magnet and striking the target. The projectile fragments produced in the target continue on through the $1m \times 2m$ drift chambers and multi-slat Time-of-Flight (TOF) wall. A small (3-in. dia.) plastic scintillation counter (DS) is used to veto non-interacting beam particles. A $20cm \times 40cm$ plastic scintillator (NS)

located just behind the TOF wall was used for the ^{15}N trigger. The NS counter was located on the high-rigidity side of the beam and had a pulse-height threshold set at the middle of the carbon fragment peak. The NaI detector was a 7 by 7 array of rectangular parallelopipeds each measuring $6.2 \times 6.2 \times 50 cm^3$. These were aligned with the long axis pointing at the target. Each element had one photomultiplier tube on the end away from the target.

A proton coincidence trigger, P, was made with a set of TOF wall slats in the region corresponding to the projectile-velocity protons. Signals from each photomultiplier tube at the top and bottom of the scintillator slat were fed into mean-timers. The output signals of the mean-timers were fed into a logic OR unit which gave a signal which indicated that one or more TOF slats fired from the region of interest. The primary trigger for this experiment was $TOT \cdot TOF_1 \cdot E_{lo} \cdot \overline{E_{hi}} \cdot \overline{HS} \cdot \overline{DS} \cdot NS \cdot P$. This requires that a beam particle be incident upon the target and that it interact before the DS scintillator and be in coincidence with the NS scintillator and with the proton-coincidence logic. The incident beam is counted as the number of particles satisfying the condition $TOT \cdot TOF_1 \cdot E_{lo} \cdot \overline{E_{hi}} \cdot \overline{HS}$ that occurred during the live time of the data acquisition system[13].

The incident beam vector and position at the target is determined from DC_3 and DC_4. The downstream particle tracks are determined by DC_1 and DC_2 and the charge is measured by pulse height in the TOF wall. The rigidity is determined from a knowledge of the magnetic field and the trajectory given by the drift chambers. Particle identification is determined by the rigidity and charge measurements. In this experiment, because we are focusing on fragments that are at low velocity in the beam rest frame, the rigidity distributions of the particles do not overlap significantly,[14] so that time-of-flight information is not necessary for particle identification.

We collected proton-energy spectra for U, Cu, Be, and blank targets. For each of these spectra the reaction rate is calculated as $R_t(E_p) = N_t(^{15}N + p, E_p)/B$, where $N_t(^{15}N + p, E_p)$ is the number of events with an $^{15}N + p$ final state with proton energy E_p for the target t, and B is the number of beam particles incident upon the target. The net target-in rate is calculated as $R'_t = R_t - R_{blank}$.

The cross sections $(d\sigma/dE_p)(mb/MeV)$ are calculated from the net rate as

$$\frac{d\sigma(t)}{dE_p} = \frac{R'_t A_t N_A}{f \rho_t d_t} \tag{6}$$

where N_A is Avogadro's number and A_t, f, ρ_t, and d_t are the atomic weight, normalization factor, density, and thickness of the target, respectively. The differential cross sections $d\sigma/dE_p$ for the U, Cu, and Be targets are shown in Fig. 2.

The normalization factor, f, accounts for the overall efficiency for reconstructing $^{15}N + p$ events. We have chosen the value of f so that

$$\int_0^{30} \left[\frac{d\sigma(U)}{dE_p} - \Gamma_U \cdot \frac{d\sigma(Be)}{dE_p} \right] dE_p = \int \sigma(\gamma, p) N_\gamma(\omega) d\omega = 82mb \qquad (7)$$

(see Eq. 3), where the parameters for calculating $N_\gamma(\omega)$ are taken from Ref. 2 and the photonuclear cross section $\sigma(\gamma, p)$ is from Refs. 9 and 10. The scaling factor Γ_U, which accounts for the different radii of U and Be, is discussed below.

III. RESULTS AND DISCUSSION

A. Cross Sections

There are two distinct regions in these cross sections, as pointed out by Webb et al.[15], the peak structure for $E_p < 20$ MeV and the smooth high-energy tail for $E_p > 20$ MeV. The high-energy tail can be attributed to a quasifree nucleon-nucleon (N-N) scattering process and is a significant part of single-nucleon knock-out reactions. The structure in the low-energy region will be the subject of the remainder of this discussion.

Webb et al. attributed the low-energy peak seen in the $^{12}C(^{12}C,^{11}B + p)X$ and $^{1}H(^{12}C,^{11}B + p)X$ reactions to a combination of nucleon-nucleus (N-A) diffractive scattering and an excitation process. For highly charged target nuclei, we expect a significant contribution resulting from the EMD process. It is clear from Fig. 2 that the low-energy cross section increases dramatically from Be to Cu to U. One can clearly see three peaks in the low-energy structure for the Cu and U targets, at 1.5, 4, and 9 MeV. The 4 and 9 MeV peaks are directly attributable to EMD. We attribute the 1.5 MeV peak to N-A diffractive scattering, which is most significant for the U target.

In our earlier studies of the EMD process[2,16] we verified the applicability of the factorization of inclusive fragmentation cross sections to permit the separation of electromagnetic and direct nuclear processes. In the present work we extend this concept and assume that N-N diffractive scattering and the EMD process are incoherent. This assumption permits us to subtract the (N-N) diffractive-scattering part of the cross section from the total cross section, leaving a combination of EMD and N-A diffractive scattering.

The method we have chosen to approximate the subtraction of the (N-N) part is to subtract the measured cross section for the Be target, scaled appropriately, from that for the Cu and U targets. That is,

$$\frac{d\sigma_{sub}(U)}{dE_p} = \frac{d\sigma(U)}{dE_p} - \Gamma_U \cdot \frac{d\sigma(Be)}{dE_p} \qquad (8)$$

where

$$\Gamma_U = \frac{\int (d\sigma(U)/dE_p) dE_p}{\int (d\sigma(Be)/dE_p) dE_p} \tag{9}$$

and the range of integration is 30 MeV $< E_p <$ 50 MeV. The scaling factors we derive are $\Gamma_{Cu} = 1.82 \pm 0.25$ and $\Gamma_U = 2.47 \pm 0.34$. These are nearly equal to the values one expects from the target-radius dependence[16], which lends confidence to this procedure. The resulting $d\sigma_{sub}/dE_p$ spectra for the U and Cu targets are shown in Fig. 3.

B. EMD and the N-A Component

After performing the subtraction described above we hypothesize that EMD and N-A diffractive dissociation are the only processes contributing to $d\sigma_{sub}/dE_p$ and we assume that these processes do not interfere with each other. In this case, for the U target we get

$$\frac{d\sigma_{sub}(U)}{dE_p} = \frac{d\sigma_{em}(U)}{dE_p} + \frac{d\sigma_{NA}(U)}{dE_p} - \Gamma_U \cdot \frac{d\sigma_{NA}(Be)}{dE_p} \tag{10}$$

We have applied the diffractive dissociation theory of Bertulani and Bauer[17] to describe the N-A diffractive dissociation cross sections, $d\sigma_{NA}/dE_p$.

For this we use Eq. 3.1 of Ref. 17 and identify the following quantities. Q is the magnitude of the 3-momentum transfer, q is the momentum of the proton relative to the ^{15}N, and R is the radius of the target nucleus. This experiment has good resolution for the relative momentum, q, but lacks resolution for the momentum transfer, Q. For our analysis we make the assumption that Q = q which implies that the momentum transfer in the diffractive dissociation process is completely absorbed by the proton. This is in agreement with the observations of Webb et al.[15]

Figure 4 shows the result of fitting the U target data with the following equation

$$\frac{d\sigma_{sub}}{dE_p} = a \cdot \frac{d\sigma_{em}}{dE_p} + b \cdot \left(\frac{d\sigma_{NA}(R_U)}{dE_p} - \Gamma_U \cdot \frac{d\sigma_{NA}(R_{Be})}{dE_p} \right) \tag{11}$$

where a, b, and R_U are the fitting parameters and we have set $R_{Be} = 1.2 \cdot A^{1/3} = 2.50 fm$. Figure 5 shows the contributions of the different terms in Eq. 11. The fit is insensitive to the radius for Be but the radius for the U target is important. The results of the fit are shown in Table 1.

TABLE I. Fit parameters from Eq. 11 for $E_p < 30MeV$.

Fitting results for the U target.	
Parameter	Value
a	0.915 ± 0.019
b	$(1.91 \pm 0.17) \times 10^{-2}$
R_U	8.90 ± 0.22 fm
χ^2/DOF	1.9

The normalization we have used for the cross sections would lead to the result of fit parameter $a = 1$ if EMD would completely describe the cross section $d\sigma_{sub}(U)/dE_p$. The fitted value for a leads us to the conclusion that N-A diffractive dissociation contributes about 8% to this cross section.

We expect that the value of R_U determined in this fit should agree with what one expects from the minimum impact parameter used for the EMD calculations (see Ref. 2) The minimum impact parameter is calculated as $b_{min} = R_{0.1}(U) + R_{0.1}(^{16}O) - d$ where the overlap parameter $d = -1.5fm$ is a result of Ref. 2. If we naively associate half of the overlap with each nucleus we get $R_U = R_{0.1} + 0.75fm = 8.67fm$. The agreement between this value and the result of fitting the present measurements verifies our assumption that $d\sigma_{sub}/dE_p$ is the sum of EMD and N-A diffractive dissociation.

The limited statistics for the Cu target data do not permit a detailed analysis as was performed for the U target data. However, the Cu cross section shown in Fig. 3 is consistent with the expected $Z_T^{1.8}$ dependence[2] of the EMD process.

C. ^{15}N Decay γ rays

The EMD theory predicts that the 9-MeV peak is due to excitation of the GDR in ^{16}O followed by decay directly to the ground state of ^{15}N, and that the 4-MeV peak results primarily from GDR decays to excited states in ^{15}N.

As a consistency check of the EMD process we positioned a 49-element NaI detector at 5° relative to the beam direction (in the lab), which could detect γ rays from the decay of excited states in ^{15}N. The solid angle acceptance of this detector was 5.5 msr (in the lab). With the kinematic focusing for 2.1 A GeV fragments, this solid angle corresponds to a 1% acceptance for ^{15}N γ rays which are emitted isotropically.

Figure 6 shows the pulse-height spectrum we obtained with the NaI detector in coincidence with the $^{16}O \rightarrow ^{15}N + p$ reactions. A 6.3-MeV γ ray from ^{15}N gets Doppler-shifted by a factor of 6 in the laboratory and therefore deposits about 38 MeV in the NaI detector. One sees that there is a broad structure in this range of the pulse-height spectrum. The energy calibration of the NaI detector was obtained

from observation of cosmic-ray muons. This spectrum is shown in Figure 7.

Figure 8 shows the $^{15}N + p$ excitation energy spectrum for the U target with and without a requirement on the NaI pulse height. The solid circles represents those events in which the NaI detector registered a pulse in the range from 25 to 60 MeV. There is a clear peak at 4 MeV for events with photons and a strong suppression of the 9 MeV peak. This is exactly what we expect for the EMD process.

IV. CONCLUSIONS

We have measured the proton energy spectra in the reaction $T(^{16}O, ^{15}N + p)X$ for the targets (T) U, Cu, and Be at 2.1 A GeV. In agreement with Webb et al.[15] we find that there is a featureless high-energy tail for $E_p > 20$MeV, which we attribute to nucleon-nucleon quasi-elastic scattering. Below 20 MeV the cross section is dominated by the electromagnetic dissociation process, for high-Z targets. An additional point of confirmation is the near absence of γ rays for events corresponding to the E_p= 9 MeV peak, because the 9-MeV peak results from the giant dipole resonance in ^{16}O decaying directly to the ground state in ^{15}N.

We have clearly demonstrated that nucleon-nucleus diffractive dissociation has a significant contribution (about 8% for the present case) to the cross section and must be considered in order to have a complete understanding of the differential cross section $d\sigma/dE_p$.

It has been pointed out many times[2,18,19] that application of EMD measurements to β-unstable nuclei would be very valuable for several reasons, not the least of which is that it would make possible the systematic delineation of the properties of the giant dipole resonance for nuclei ranging from one to several nucleons removed from the valley of β-stability. The question has been whether beams of β-unstable nuclei could be produced that are intense enough to make possible such studies. In the present work, we had to reduce the ^{16}O beam intensity at the Bevalac from its normal value by a factor of $\sim 10^5$ in order to achieve counting rates nearly free from pile-up. Thus, we have clearly shown with these exclusive cross-section measurements that the EMD process can be exploited to yield exciting possibilities for studying photonuclear reactions for both stable and β-unstable nuclei, and thus to open up a new and potentially very fruitful field of nuclear physics.

V. ACKNOWLEDGMENTS

We would like to thank Harry Heckman for his inspiring interest and pioneering efforts leading to this work. Additionally we would like to acknowledge many stimulating discussions with the late Abe Goldberg.

This work is supported by DOE Contracts DE-AC03-76SF00098, DE-FG05-86ER40285, NSF Grant PHY81-21003, and NASA Grant NGR-05-003-513.

---

[1]H. H. Heckman and P. J. Lindstrom, Phys. Rev. Lett. **37**, 56 (1976).

[2]D. L. Olson, B. L. Berman, D.E. Greiner, H. H. Heckman, P. J. Lindstrom, G. D. Westfall, and H. J. Crawford, Phys. Rev. C **24**, 1529 (1981).

[3]L. Ramello, Z. Phys. C**38**, 73 (1987).

[4]C. Brechtman and W. Heinrich, Z. Phys. A **330** 407 (1988); C. Brechtman and W. Heinrich, Z. Phys. A **331** 463 (1988); C. Brechtman, W. Heinrich, and E. V. Benton, Phys. Rev. C **39** 2222 (1989).

[5]P. B. Price, R. Guoxiao, and W.T.William, Phys. Rev. Lett. **61** 2193 (1988).

[6]I. Tanihata, Nucl. Phys. **A488** 113c (1988).

[7]J. Barrette, P. Braun-Munzinger, W. E. Clelend, G. David, E. Duek, M. Fatyga, D. Fox, S. V. Greene, J. R. Hall, R. Heifetz, T. K. Hemmick, N. Herrmann, R. W. Hogue, G. Ingold, K. Jayananda, D. Kraus, A. Legault, D. Lissauer, W. J. Llope, T. Ludlum, R. Majka, D. Makowiecki, S. K. Mark, J. T. Mitchell, M. Muthuswamy, E. O'Brien, L. H. Olsen, V. Polychronakos, M. Rawool-Sullivan, F. S. Rotondo, J. Sandweiss, B. Shivakumar, J. Simon, U. Sonnadara, J. Stachel, J. Sunier, H. Takai, T. G. Throwe, H. VanHecke, L. Waters, W. J. Willis, K. Wolf, D. Wolfe, and C. L. Woody, Phys. Rev. C **41**, 1512 (1990).

[8]J. C. Hill, M. T. Mercier, F. K. Wohn, and A. R. Smith, Phys. Rev. Lett. **52**, 898 (1984), M. T. Mercier, J. C. Hill, F. K. Wohn, C. M. McCullough, M. E. Nieland, J. A. Winger, C. B. Howard, S. Renwick, and D. K. Matheis, Phys. Rev. C **33**, 1655 (1986), J. C. Hill, F. K. Wohn, J. A. Winger, and A. R. Smith, Phys. Rev. Lett. **60** 999 (1988), J. C. Hill, F. K. Wohn, J. A. Winger, M. Khayat, K. Leininger, and A. R. Smith, Phys. Rev. C **38** 1722 (1988), J. C. Hill, F. K. Wohn, J. A. Winger, M. Khayat, M. T. Mercier, and A. R. Smith, Phys. Rev. C **39** 524 (1989)

[9]J. T. Caldwell, (PhD thesis, University of California), (1967) UCRL-50287.

[10]J. T. Caldwell, S. C. Fultz, and R. L.Bramblett, Phys. Rev. Lett. **19**, 447 (1967).

[11]J. E. E. Baglin and M. N. Thompson, Nucl. Phys. **A138**, 73 (1969).

[12]R. C. Morrison, PhD thesis, Yale University (1965).

[13]J. Engelage, M. E. Baumgartner, E. Beleal, B. L. Berman, F. Bieser, F. P. Brady, M. Bronson, J. B. Carroll, H. J. Crawford, I. Flores, D. E. Greiner, L. Greiner, O. Hashimoto, G. Igo, S. Kadota, P. N. Kirk, P. J. Lindstrom, C. McParland, S. Nagamiya, D. L. Olson, J. Porter, J. L. Romero, C. L. Ruiz, T. J. M. Symons, I. Tanihata, R. Wada, M. L. Webb, J. Yamada, and H. Yee, Nucl. Instrum. Methods A**277** 431 (1988).

[14]D. E. Greiner, P. J. Lindstrom, H. H. Heckman, Bruce Cork, and F. S. Bieser, Phys. Rev. Lett. bf 35), 152 (1973).

[15]M. L. Webb, H. J. Crawford, J. Engelage, M. E. Baumgartner, D. E. Greiner, P. J. Lindstrom, D. L. Olson, and R. Wada, Phys. Rev. C**36**, 193 (1987).

[16]D. L. Olson, B. L. Berman, D. E. Greiner, H. H. Heckman, P. J. Lindstrom, and H. J. Crawford, Phys. Rev. C**28**, 1602 (1983).

[17]C. A. Bertulani and G. Bauer, Nucl. Phys. A**480** 615 (1988).

[18]B.L. Berman in Proc. Symp. on Perspectives in Electro- and Photonuclear Physics, CEN Saclay, 7 (1980), B.L. Berman in Proc. Workshop on Prospects for Research with Radioactive Beams from Heavy Ion Accelerators, Washington D.C., 92 (1984).

[19]I. Tanihata, H. Hamagaki, O. Hashimoto, S. Nagamiya, Y. Shida, N. Yoshikawa, O. Yamakawa, K. Sugimoto, T. Kobayashi, D. E. Greiner, N. Takahashi, and Y. Nojiri, Phys. Lett. **160B**, 380 (1985), I. Tanihata, H. Hamagaki, O. Hashimoto, Y. Shida, N. Yoshikawa, K. Sugimoto, O. Yamakawa, T. Kobayashi, and N. Takahashi, Phys. Rev. Lett. **55**, 2676 (1985), I. Tanihata, RIKEN-AF-NP-58 (1987), I. Tanihata, Nucl. Phys. A**488** 113c (1988).

FIG. 1. A schematic view of the experimental setup.

FIG. 2. The measured exclusive fragmentation cross section as a function of proton energy for U, Cu and Be targets. The proton energy is measured in the PF rest frame.

FIG. 3. The Be-subtracted cross sections ($d\sigma_{sub}/dE_p$) for U and Cu targets.

FIG. 4. The result of fitting Eq. 11 to the Be-subtracted U target cross section.

FIG. 5. The contributions of the different terms on the right-hand-side in Eq. 11. EMD denotes first term, U denotes second term, Be denotes the third term, and U-cBe denotes combined second and third terms.

FIG. 6. Laboratory photon energy spectrum in the NaI detector for all $^{15}N + p$ events.

FIG. 7. The energy calibration spectrum for the NaI array using comsic ray muons. This corresponds to the energy deposited in one cell.

FIG. 8. The crosses show the total excitation energy spectrum for the U target and the solid circles the same spectrum from events for which the NaI detector registered a pulse between 25 and 60 MeV. The two curves are normalized to the same area for the 4 MeV peak. Note that the excitation energy is approximately 16/15 times the proton energy.

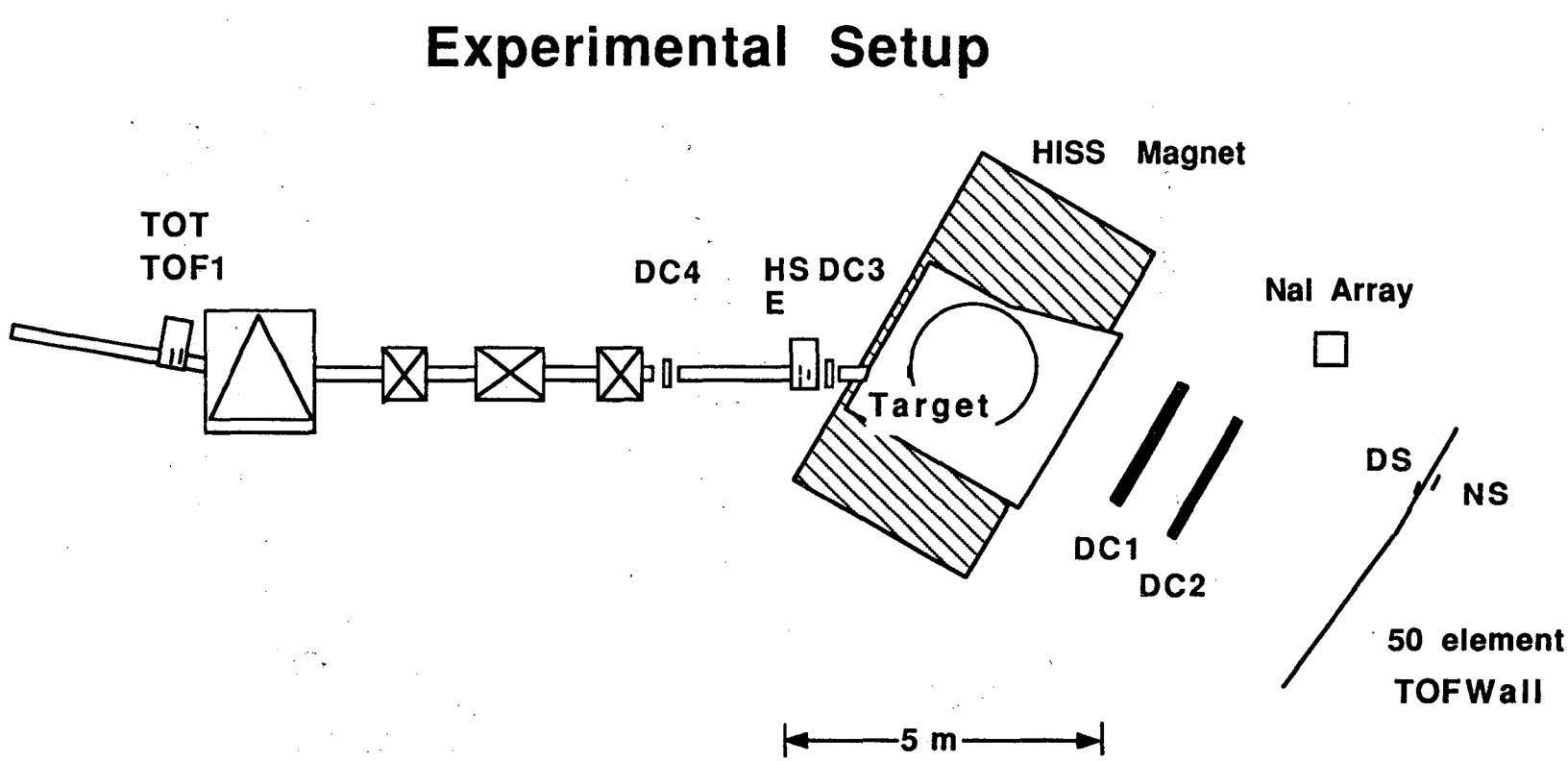
Experimental Setup
HISS Magnet
TOT
TOF1
DC4
HS
E
DC3
Nal Array
Target
DS
NS
DC1
DC2
50 element
TOFWall
5 m

Figure 1.

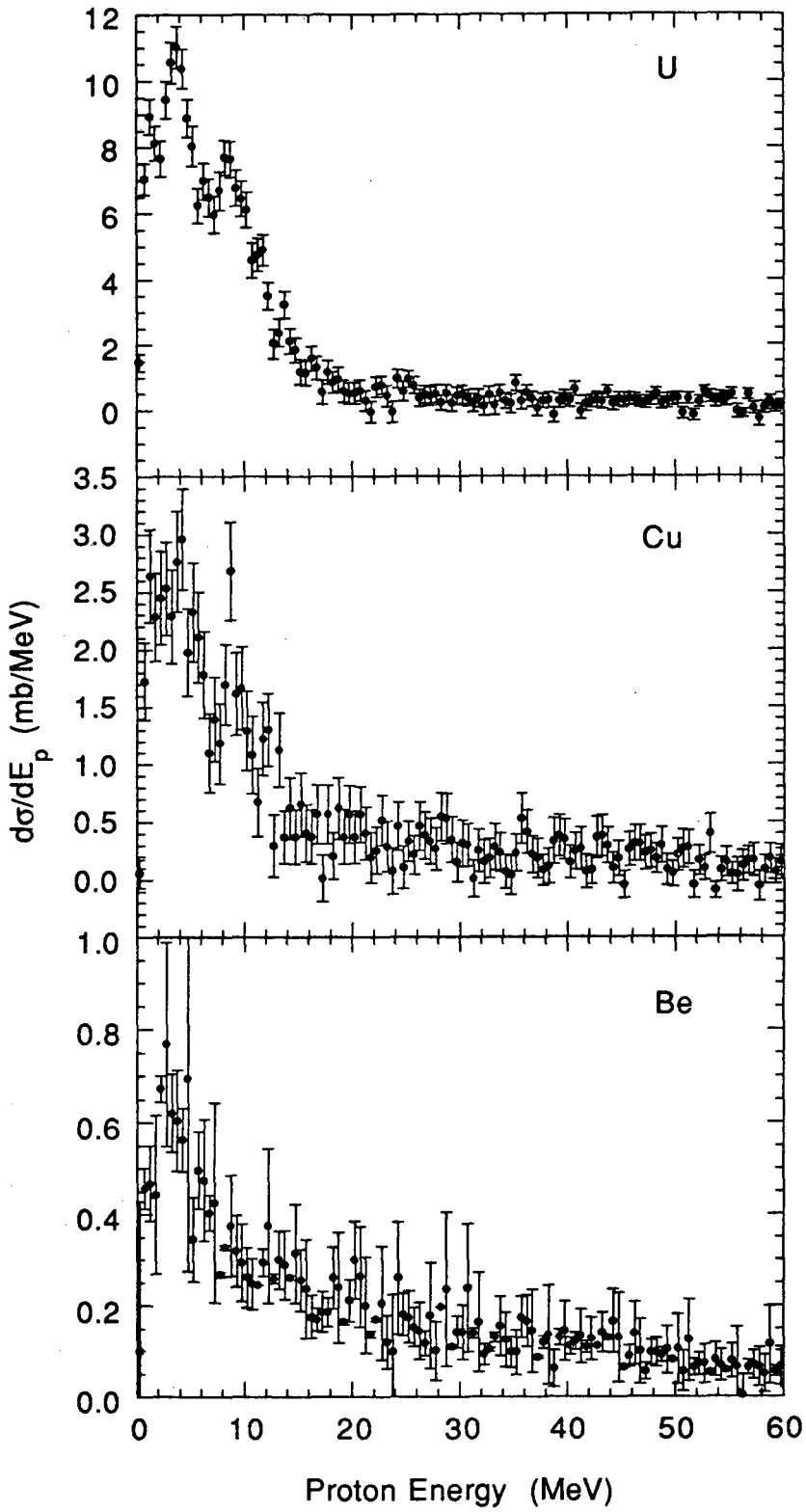

Figure 2.

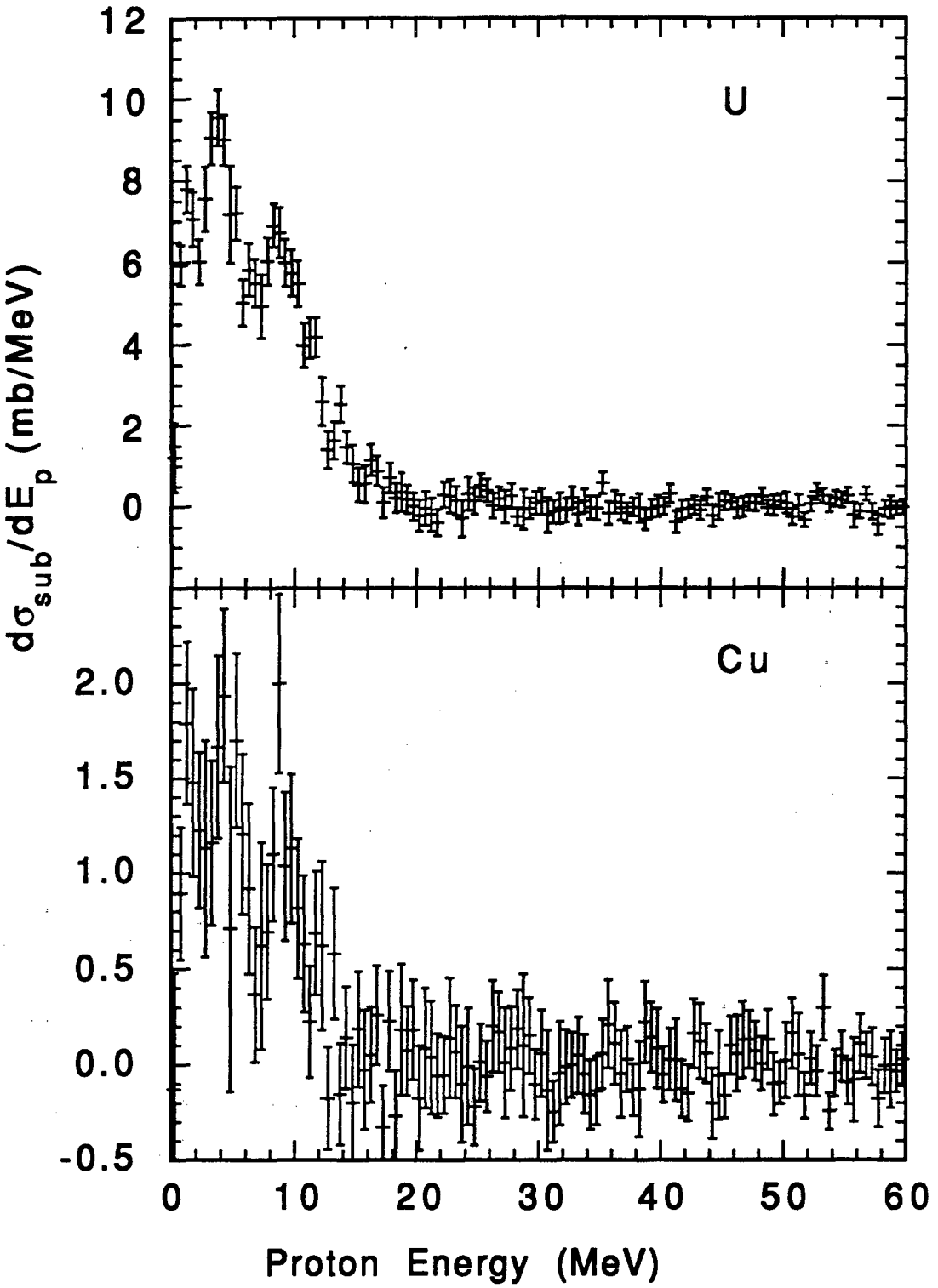
U
Cu
$d\sigma_{sub}/dE_p$ (mb/MeV)
Proton Energy (MeV)
12
10
8
6
4
2
0
2.0
1.5
1.0
0.5
0.0
-0.5
0
10
20
30
40
50
60

Figure 3.

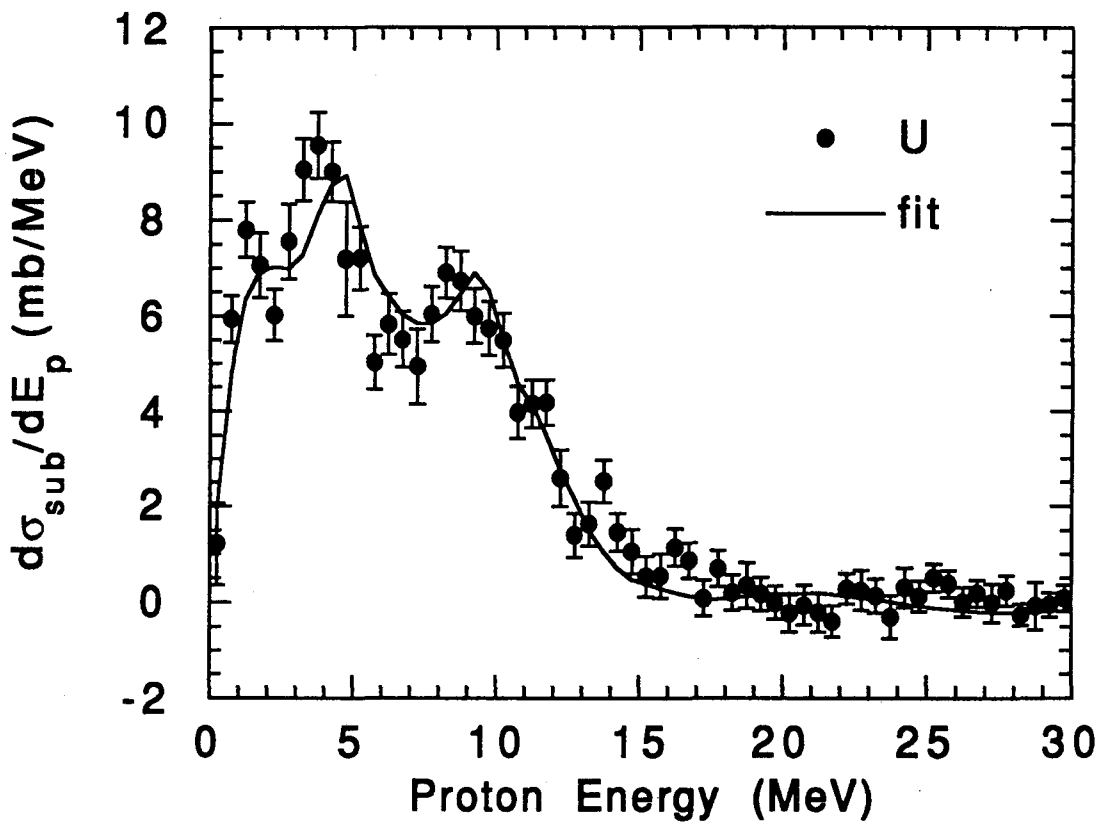
12
10
8
6
4
2
0
-2
0
5
10
15
20
25
30
$d\sigma_{sub}/dE_p$ (mb/MeV)
Proton Energy (MeV)
U
fit

Figure 4.

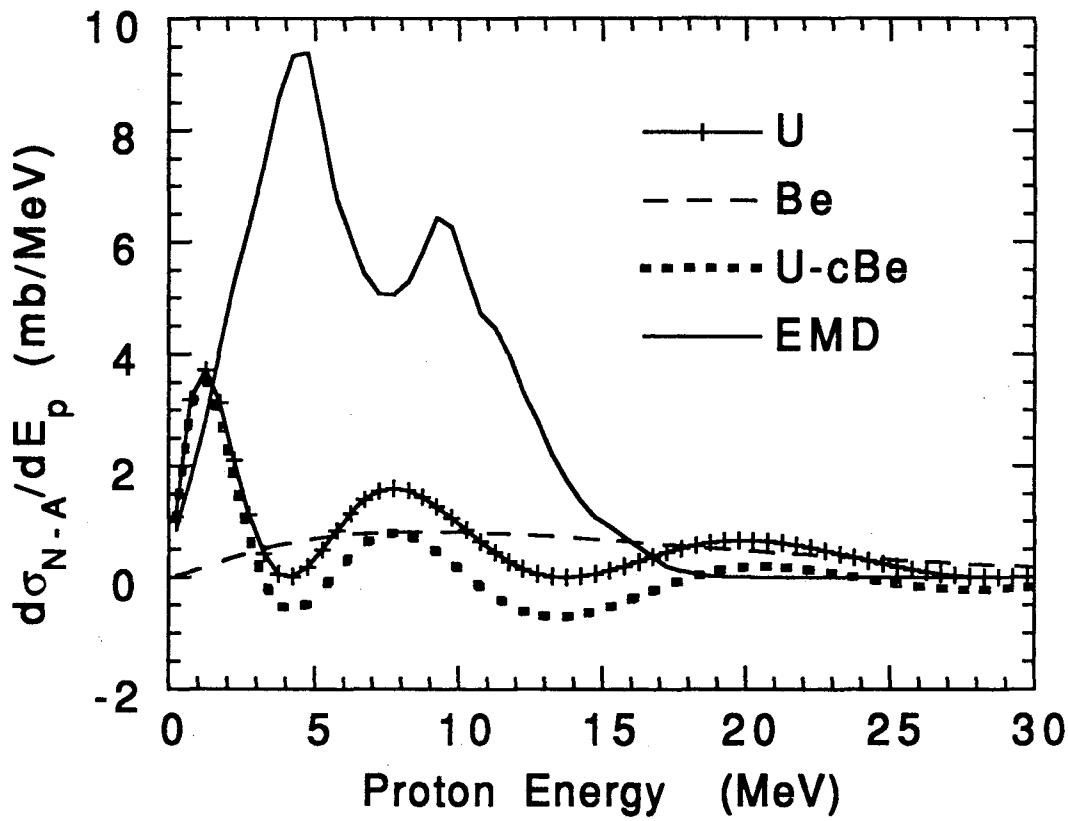
10
8
6
4
2
0
-2
0
5
10
15
20
25
30
$d\sigma_{N-A}/dE_p$ (mb/MeV)
Proton Energy (MeV)
U
Be
U-cBe
EMD

Figure 5.

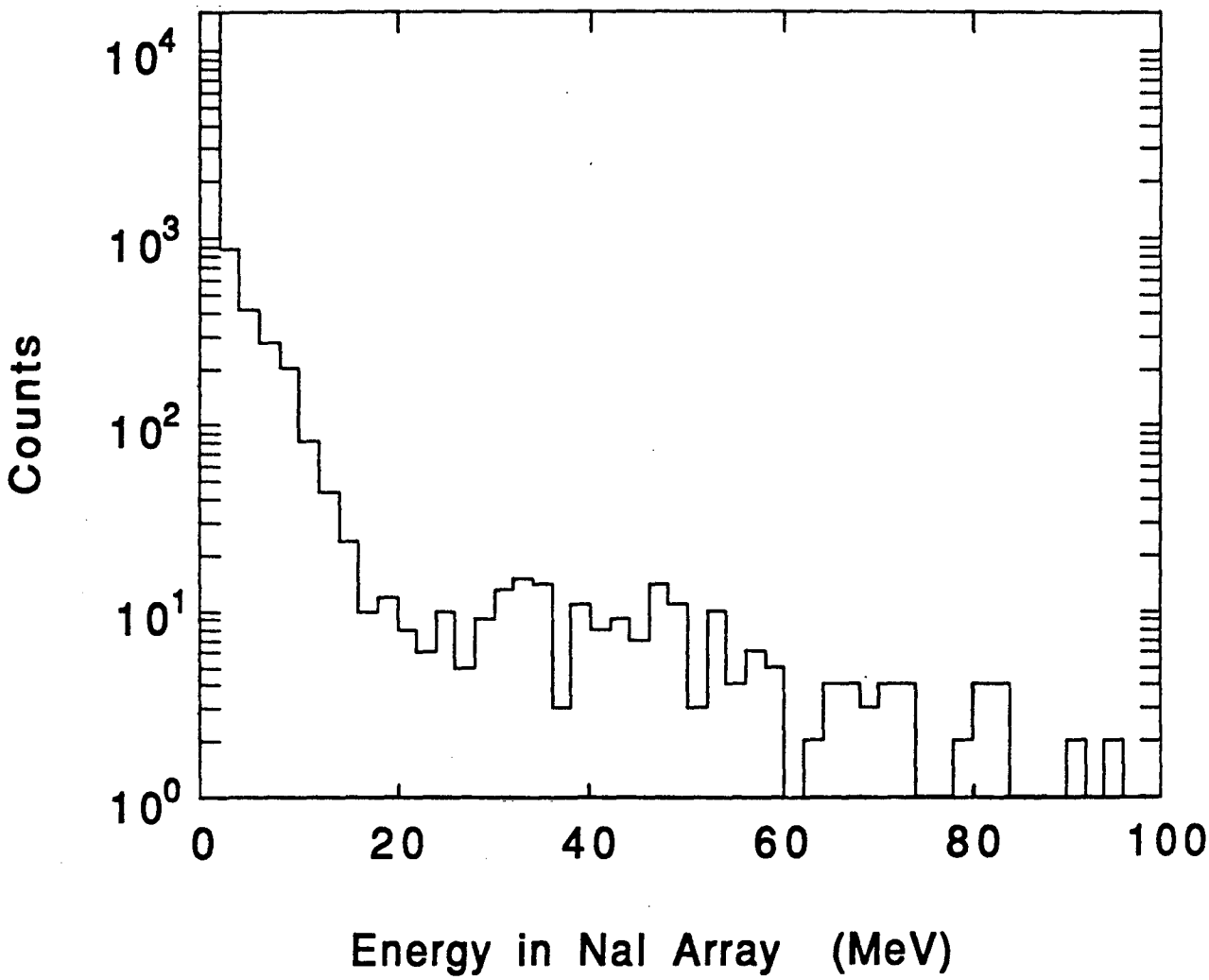
Counts
10^4
10^3
10^2
10^1
10^0
0
20
40
60
80
100
Energy in NaI Array (MeV)

Figure 6.

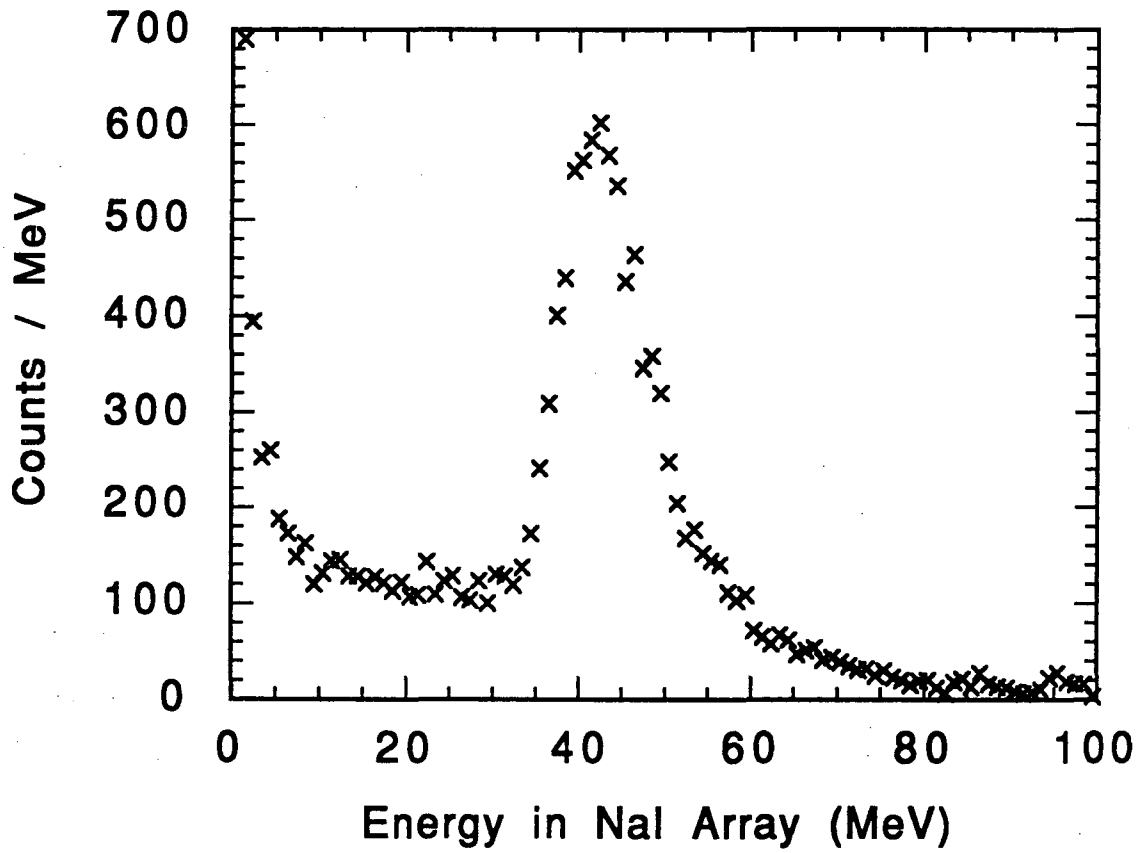
700
600
500
400
300
200
100
0
Counts / MeV
0
20
40
60
80
100
Energy in NaI Array (MeV)

Figure 7.

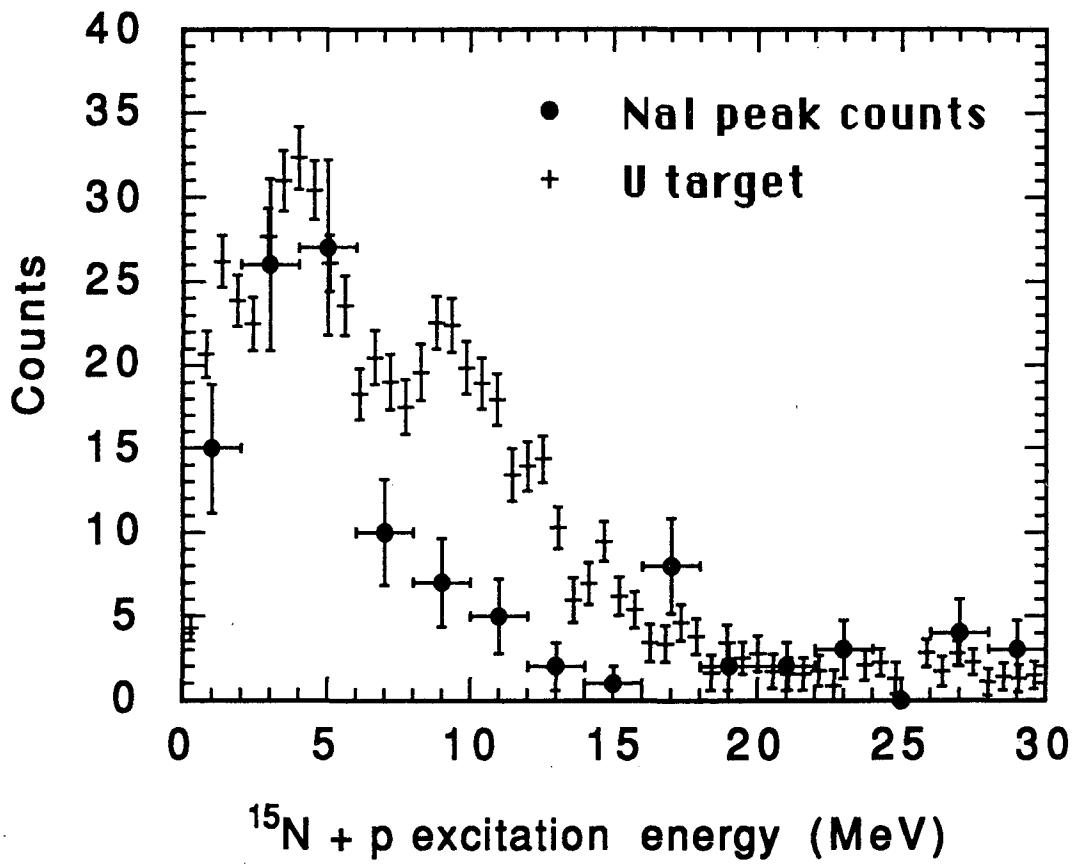
40
35
30
25
20
15
10
5
0
Counts
NaI peak counts
U target
0
5
10
15
20
25
30
15N + p excitation energy (MeV)

Figure 8.

LAWRENCE BERKELEY LABORATORY
UNIVERSITY OF CALIFORNIA
INFORMATION RESOURCES DEPARTMENT
BERKELEY, CALIFORNIA 94720